Title

Unraveling the Dynamics of Burn Wound Healing in Murine Model: Insights into Immune Signaling Pathways, Tissue Regeneration, and Biomaterial-Based Therapies

Author

Hsu, Wilson

Publication Date

2024

Peer reviewed|Thesis/dissertation

UNIVERSITY OF CALIFORNIA

Los Angeles

Unraveling the Dynamics of Burn Wound Healing in Murine Model: Insights into Immune Signaling Pathways, Tissue Regeneration, and Biomaterial-Based Therapies

A thesis submitted in partial satisfaction

of the requirements for the degree Master of Science

in Bioengineering

by

Wilson Hsu

2024

ABSTRACT OF THE THESIS

Unraveling the Dynamics of Burn Wound Healing in Murine Model: Insights into Immune Signaling Pathways, Tissue Regeneration, and Biomaterial-Based Therapies

by

Wilson Hsu

Master of Science in Bioengineering

University of California, Los Angeles, 2024

Professor Philip O. Scumpia, Co-Chair

Professor Dino Di Carlo, Co-Chair

This study investigates wound healing differences between full-thickness excisional wounds and scald burns in adult mice, highlighting the challenges of burn injury regeneration. Despite timely debridement, burns consistently exhibit delayed healing and increased scarring compared to excisional wounds. We develop a mouse model that recapitulates the clinical features of burn wounds in humans. We use this model to explore the potential of D-peptide and L-peptide crosslinked microporous annealed particle (MAP) hydrogels to enhance burn wound

regeneration. Our findings underscore the critical influence of injury mechanisms on tissue regenerative potential, suggesting that MAP hydrogels, particularly those with peptide crosslinking would improve burn wounds. These insights deepen our understanding of wound healing dynamics. Our findings reveal the therapeutic strategies to enhance tissue repair and regeneration in burn injuries, ultimately advancing clinical interventions and improving patient care.

The thesis of Wilson Hsu is approved.

Song Li

Philip O. Scumpia, Committee Co-Chair

Dino Di Carlo, Committee Co-Chair

University of California, Los Angeles

2024

Dedicated to my parents, Richard Hsu and Wendy Lu,

for the superpowers to make anything come true.

ACKNOWLEDGEMENTS

I would like to express my heartfelt gratitude to my advisor, Dr. Philip O. Scumpia. His exceptional leadership and insightful advice have significantly contributed to my growth over the past two years of pursuing my Master's degree. His unwavering support, patience, and guidance have been invaluable, and I am deeply thankful for his mentorship. Dr. Scumpia's vast knowledge and visionary approach introduced me to an incredible research field. His optimism and enthusiasm for research have consistently motivated me to strive for excellence every day. I am profoundly grateful to have had Dr. Scumpia as my advisor.

I would also like to thank the other committee members sincerely, Dr. Song Li and Dr. Dino Di Carlo. Their guidance has broadened my perspectives and allowed me to explore various facets of my research topic. Their advice has been instrumental in refining my project and enhancing its technical aspects.

I am also grateful to all the members of the Scumpia Lab for their support and valuable insights. I would like to thank Iqra Arshad for collaborating, providing guidance through numerous experiments and projects, and helpful insight into everything.

Finally, I would like to thank my parents, Dr. Richard Hsu and Mrs. Wendy Lu, for their unwavering support and encouragement throughout my academic journey. Their guidance has been pivotal in helping me achieve my goals.

TABLE OF CONTENTS

LIST OF FIGURES

INTRODUCTION

A full-thickness burn, often called a third-degree burn, is a severe injury that extensively damages the outer and inner skin layers and the underlying fat, and nerves [1]. These burns are classified as medical emergencies and generally do not heal without medical treatment. They are distinct in that they often impair nerves, resulting in reduced or absent pain sensation compared to first and second-degree burns[2].

In humans, performing early excision for burn patients between post-burn days 2 and 12 is a crucial surgical intervention during hospitalization[3]. Timely burn debridement is pivotal in improving the overall chances of survival and the outcome for burn victims. It is essential to promptly remove eschars and blisters to halt the inflammatory cascade, which can lead to secondary damage. Burned and dead tissue in full-thickness burns creates an environment conducive to gram-positive cellulitis, resulting in delayed healing, physiological challenges, contractures, and functional limitations. Burn patients undergoing early excision lead to reduced hospitalization duration and quicker wound healing[4].

Sebaceous glands are small, specialized structures located within the skin, primarily in the dermis, which is the deeper layer of the skin[5]. These glands are responsible for maintaining the health and function of the skin. Sebaceous glands are responsible for producing sebum, secreted onto the skin's surface through hair follicles. Sebaceous glands are typically associated with hair

follicles adjacent to them within the skin[6].

One thing to remember about the difference between human and mouse skin is that human skin doesn't appear to have sebaceous glands regenerating in excisional and burn wounds. In mice, wound-induced hair neogenesis regenerates sebaceous glands in large excisional wounds but not burn wounds[7]. Wound-induced hair neogenesis is unexplored in other wounds and absent in humans. This intricate process involves epithelial-mesenchymal cell interactions, mainly influenced by Wnt signaling, with inflammation playing a crucial role in tissue and hair follicle regeneration[8].

Therefore, we delve into the intricate mechanisms governing wound healing, mainly focusing on the interplay between Toll-like receptor (TLR) signaling pathways in macrophages[9]. Previous studies have illuminated the pivotal role of Myeloid differentiation primary response 88 (MyD88) and TIR-domain-containing adapter-inducing interferon-β (TRIF) in orchestrating the switch of macrophages from an inflammatory to an angiogenic phenotype, which is crucial for effective wound repair[10]. Building upon this foundation, we embarked on burn wound experiments utilizing MyD88-TRIF knockout mice to unveil further insights into wound healing dynamics. By comparing the healing process in these genetically modified mice to that in wild-type counterparts, we seek to elucidate the impact of adaptive immune responses on the wound healing cascade.

In recent years, injectable biomaterials have shown promise for tissue regeneration, yet traditional hydrogels face limitations due to their reliance on gel degradation before tissue reformation. Introduced in 2015, interconnected microporous annealed particle (MAP) scaffolds offer a solution by providing simultaneous tissue reformation and material degradation support. Through precise engineering of monodisperse micro-gel building blocks via microfluidic formation, MAP scaffolds offer tailored physical and chemical properties. Previous studies demonstrate their ability to promote rapid cell proliferation and 3D network formation in vitro and expedite tissue regeneration in vivo. Particularly promising is their application in burn injuries, where heightened fibrosis poses a significant challenge to wound healing. Incorporating peptide crosslinking further enhances their potential for wound regeneration. These advancements underscore the critical influence of injury mechanisms on tissue regenerative potential, emphasizing the need for innovative approaches in addressing complex tissue regeneration challenges[11].

Further investigation on slowing MAP degradation by transitioning crosslinking peptides from L- to D-amino acids, aiming for enhanced tissue ingrowth before scaffold degradation. Surprisingly, while D-peptide crosslinked MAP hydrogel (D-MAP) demonstrated anticipated slower enzymatic degradation in vitro, it unexpectedly accelerated material degradation in vivo. Nonetheless, D-MAP facilitated tissue regeneration in healed cutaneous wounds, enhancing

tensile strength and promoting hair neogenesis. Moreover, MAP scaffolds recruited IL-33 type 2 myeloid cells, with amplification in the presence of D-peptides. D-MAP induced notable antigen-specific immunity against D-chiral peptides, with intact adaptive immunity crucial for hydrogel-induced skin regeneration. These findings underscore the capacity of biomaterial-induced adaptive immune responses to drive cutaneous regenerative healing despite accelerated scaffold degradation[12].

This study aims to delve into the intricate mechanisms underlying the phenomenon of full-thickness burns, characterized by profound damage to the skin layers. Early excision, a critical surgical intervention within a specific timeframe post-burn injury, is pivotal in enhancing patient outcomes by averting secondary damage and fostering expedited wound healing. In a addition, we explore the essential role of sebaceous glands, which are integral to skin health and wound regeneration. While sebaceous gland regeneration in excisional wounds is observed in mouse models, such regenerative capacity is notably absent in human burn wounds, highlighting a significant interspecies variation that warrants investigation into the underlying mechanisms. Through elucidating these complex interactions, this study aims to contribute insights crucial for advancing therapeutic strategies in burn wound management and optimizing patient care.

Furthermore, we aim to investigate the comparative efficacy of Solosite™, a known wound-healing product, with newly developed MAP gels containing D-MAP hydrogel and L-MAP

hydrogel. Our primary focus is to discern differences among these products in facilitating wound healing. Additionally, we endeavor to explore their effects on the regeneration of sebaceous glands, which are crucial for comprehensive tissue recovery. This research builds upon the understanding that burn wounds exhibit slower healing rates and lack sebaceous gland regeneration compared to excisional wounds. By conducting this follow-up experiment, we seek to contribute insights into optimizing wound care strategies, potentially identifying the most effective product for promoting wound closure and sebaceous gland regeneration. Such findings could significantly impact clinical practice, offering improved therapeutic options for individuals suffering from various types of wounds, particularly burns.

METHODS

Animals

Animals for the experiments are C57BL/6J mice from the Jackson Laboratory, Bar Harbor, ME, aged 8 to 12 weeks and weighing 16 to 20 g. Animals were assigned to scald burn or sham (control) groups. All sham mice were excised in a 1.6 cm*1.6 cm wound on the lower dorsal area. Group of scald burn mice were further assigned to subgroups in different experiments. In the delayed excision experiment, the mice were divided into 1.5 cm*1.5 cm burn wound debride at 1 hr, 4 hr, and 24 hr postburn in the same excisional size of 1.6 cm*1.6 cm on the lower dorsal area, with 7 mice per group. In the different-size excision experiment, the mice were divided into a group of 1 cm*1 cm burn wound and 1.5 cm*1.5 cm burn wound excisions 24 hours postburn in 1.6 cm*1.6 cm of wound size, with 5 mice per group. In the MAP gel experiment, the mice were divided into L-MAP, D-MAP, and Solosite™ groups 24 hours postburn in 1.6 cm*1.6 cm of wound size, with 4 mice per group.

Scald/Sham burn mouse model

The experiments used animal tissues aligned with the Chancellor's Animal Research Committee (ARC) ethical guidelines at UCLA under protocol # 10–011 (skin wound healing model) for sham wound group and under protocol # 15-031 (immunomodulatory porous biomaterials for regenerative healing of burn wounds) for burn wound. A mouse burn wound

model was performed on C57BL/6J mice (Jackson Laboratories) ranging from 8 to 12 weeks old. The mice were anesthetized during the procedure using 5 vol% aerosolized isoflurane for induction and 5 vol% aerosolized isoflurane for maintenance. The dorsal side of the mice was shaved using electric clippers and then disinfected with serial washes of povidone-iodine and 70% ethanol. 0.05mg/mL of buprenorphine was injected intramuscularly. A mold was created by cutting a 1.5 cm*1.5 cm square on the cap of a 50mL plastic centrifuge tube, and the bottom of the tube was cut to create an opening for pouring water. In addition to the different-size wound experiment, a 0.9cm*0.9cm size mold was also made. The mold was placed on a clamp stand to ensure precise placement and tightness on the dorsal side of the mice. To form the scald burn, tap water was boiled in an electric kettle and brought to a boiling point of 100℃; then 10mL was poured through the mold onto the dorsal side of the mice. Sham wounds were generated by pouring room-temperature water through the mold instead of boiling water. Suction was used to retrieve the water from the mold after contacting the mice's skin for 6, 8, or 10 seconds to determine full-thickness burn (following experiments were done by performing 8-second scald burns). After the wound was made, the mice were placed on a warm electric pad to prevent hypothermia and then placed in their cage. Mice were housed 5 mice in one cage. Each mouse's weight was monitored daily to avoid dehydration, and 1 mL of normal saline was injected subcutaneously if the weight loss was over 10% of the original weight. The mice were observed

for 28-31 days following harvesting of the scar area. MyD88-TRIF knockout burn mouse model follows the same procedure but is observed for a more extended period (35-42 days) for a slower wound closure.

Evaluation of wound closure

To follow the closure of the wounds, mice were imaged on designated days with a Canon EOS 2000D high-resolution camera with an 18-55mm lens. The wound area was determined by comparing the pixel area, measured through ImageJ, with the pixel area of a ruler measuring 1 cm. Closure rates were compared to Day 0 for each sample.

Tissue Collection

Following the healing of wounds, mice were sacrificed on the specified day post-injury, and tissue was gathered with an approximate 5mm margin surrounding the healed wound. The tissue was fixed with 4% paraformaldehyde for 24 hours, washed with 1X PBS twice, and kept at 4C until sectioned with cryostat or microtome.

Histology

Tissue samples were sectioned 4um thick and stained with hematoxylin and eosin. A board-certified dermatopathologist analyzed the sections to determine full-thickness burns and cell profiles of the wounds. The Translational Pathology Core Laboratory in the Department of Pathology & Laboratory Medicine at David Geffen School of Medicine at UCLA performed the

paraffin embedding of tissues.

Sebaceous gland quantification

Following the previous tissue collection procedures, tissue was harvested with Oil red O staining to identify the sebaceous glands. Oil Red O (ORO) is a fat-soluble dye that stains neutral lipids, cholesteryl esters, and lipoproteins, which can indicate the presence of sebaceous glands. ORO stock solution was premade with 0.3g ORO powder in 100 mL of isopropanol, then filtered once using KimWipes. Before staining, ORO working solutions were made freshly, with a stock ORO to ddH_2O racial of 3:2, mixed and filtered using KimWipes. 400 µL of ORO working solution was added to the tissue and was set to room temperature for an hour. The tissue was later rinsed with running water in a bucket by dipping in and out for 5 to 10 minutes. The tissue was left to dry overnight and will be observed under a microscope to quantify the amount of the sebaceous gland.

Microporous Annealed Particle (MAP) hydrogel fabrication

Two aqueous solutions were prepared to facilitate microgel formation. One solution comprised 10% w/v four-arm polyethylene glycol–vinyl sulfone (20 kDa, JenKem) in 300 mM triethanolamine (Sigma), pH 8.25, prefunctionalized with a mixture of 500 µM K-peptide (Ac-FKGGERCG-NH2) (GenScript), 500 µM Q-peptide (AcNQEQVSPLGGERCG-NH2), and 1 mM RGD (Ac-RGDSPGERCG-NH2) (GenScript). The other solution contained: (1) 8 mM

dicysteine-modified MMP substrate (Ac-GCRDGPQGIWGQDRCG-NH2) (GenScript) with all l-chirality amino acid residues for l-MMP microgel, or (2) d-chirality amino acid substitutions at the site of MMP-mediated recognition and cleavage (Ac-GCRDGPQDGIDWDGQDRCG-NH2) for d-MMP microgels. The oil phase consisted of heavy mineral oil (Fisher) containing 0.25% v/v Span-80 (Sigma). The two solutions were combined in the droplet generator and immediately formed monodisperse droplets upon pinching. Downstream of the pinching region, a second oil inlet with a high concentration of Span-80 (5% v/v) was introduced to the flowing droplet emulsion. Both aqueous solution flow rates were set at 2.5 µl /min, while oil solutions flowed at 20 µl/min. The mixture underwent an overnight reaction at room temperature. It was purified by repeated washes with HEPES-buffered saline pH 7.4, followed by pelleting in a tabletop centrifuge at 18,000g for 5 min. Particles were washed with equal volumes of 1X PBS and 2 mL of hexane, centrifuged at 18,000g for 2.5 min, and the supernatant was removed. The washing process will be repeated until the particles are swallowed 3 times to their original size.

MAP hydrogel burn mouse model

The experiments used animal tissues aligned with the Chancellor's Animal Research Committee (ARC) ethical guidelines at UCLA under protocol # 15-031 (immunomodulatory porous biomaterials for regenerative healing of burn wounds). We follow the same procedure of would formation as scald/sham burn mouse model. After the burn site was However, mice were

single-housed instead of 5 in a cage in the MAP hydrogel experiment to prevent them from scratching off the wrap. Annealing commenced by combining equal volumes of the building block solutions containing thrombin and FXIII utilizing a positive displacement pipette (Gilson) before applying. These solutions were thoroughly mixed by repetitive pipetting up and down while simultaneously stirring with the pipette tip. The resulting mixture was subsequently pipetted onto the wound. Mice were initially applied with 200 μL of MAP hydrogel (D-MAP or L-MAP) or Solosite™ according to different control groups individually. Tegaderm was applied to the wound area after MAP hydrogel or Solosite™ application with double-sided Tegaderm right at the wound to avoid direct adhesion onto the MAP hydrogel or Solocite. Coban was wrapped over the torso of the mouse to prevent the Tegaderm from loosening and being bitten by the mouse. Coban and Tegaderm were changed every 3 days to monitor wound closure and avoid infection, and 50 μL of 1X PBS was applied to the mouse with MAP hydrogel to prevent it from drying. 200 μL of Solosite™ was applied every 3 days instead of 1X PBS for the Solosite™ group. Coban and Tegaderm changing and PBS/ Solocite reapplication will stop as soon as the wound is fully healed. The mice were observed for 28-31 days following harvesting of the scar area.

Statistical analysis

Statistical distinctions were assessed through two-way repeated measures ANOVA with

subsequent pairwise comparisons and Tukey–Kramer adjustment, facilitated by GraphPad Prism software. Data were expressed as mean values accompanied by the standard error of the mean. Significance was denoted by $p < 0.05$.

RESULTS

Burn wounds show delayed healing compared to sham wounds

Our observations revealed a striking distinction in investigating the variance in wound healing between sham and scald burn wounds subjected to debridement 24 hours post-injury. Following the procedure shown in Figure 1a, Figure 1b shows that on day 0, sham and scald burn wounds exhibited comparable characteristics. However, a noticeable discrepancy emerged by day 9, with sham wounds displaying accelerated healing compared to full-thickness scald burns, which remained open. Remarkably, by day 15, sham wounds had completely healed, while full-thickness scald burn wounds still exhibited significant openness. Figure 1c delineating these distinctions underscores a pivotal point on day 6, with the most notable contrast occurring by day 9, suggesting a substantial delay in burn wound closure compared to sham wounds. As the study progressed, around day 17, the dissimilarity between excisional and full-thickness scald burn wounds diminished, reflecting the burns' proximity to full healing.

Continuing our investigation within the same experiment, we examined the impact of debridement timing on burn wound healing, assessing interventions at 1, 4, and 24 hours post-injury (Figure 1d). Our findings revealed no significant disparity in wound healing across these different debridement time points, according to Figure 1e.

In Figure 1f, our analysis unveiled a noteworthy finding in examining the sebaceous gland

count between sham and burn wounds subjected to excision at three distinct time points (1 hour, 4 hours, and 24 hours post-injury). Specifically, a significant disparity in sebaceous gland count was evident between sham and burn wounds in the scar tissue. However, no discernible variance in sebaceous gland count was observed among the different time points of excision within the burn wound group (1 hour, 4 hours, and 24 hours post-injury). This observation suggests that the timing of debridement, whether early or delayed, did not exert a discernible effect on the overall wound healing trajectory in burns. These results contribute valuable insights into the dynamics of wound healing post-burn injury, shedding light on the natural course of healing and the efficacy of timely debridement interventions.

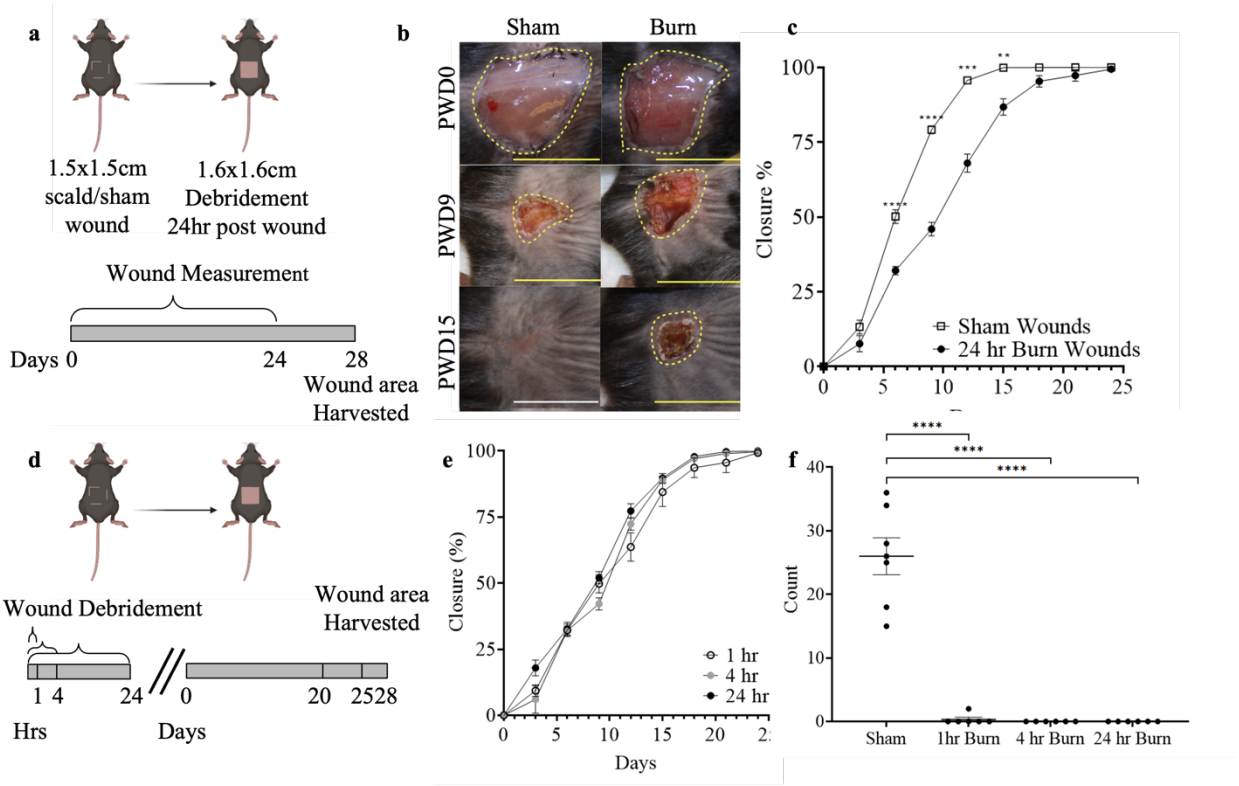

Figure 1: Burn wounds show delayed healing compared to sham wounds, regardless of whether burn wounds were debrided early or later. a) Both excisional and burn wounds were debrided in a 1.6 cm*1.6 cm size wound, and wound size was kept track until fully healed. b) Wound size comparison for two different groups: sham wounds and burn wounds. Pictures show changes in the wound at four time points: procedure day (Day 0), the most significant difference in closing rate (Day 9), and sham wound fully closed (Day 15). c) Different wound closure rates of sham and burn wounds from day 0 to day 24. After the procedure, the wound closure percentage started to significantly differ on day 6, with the most significant difference on day 9. Most sham wounds closed on day 15, while most burn wounds closed on day 22. d) Assessment experiment procedure on the impact of debridement timing on burn wound healing at 1, 4, and 24 hours post-injury. e) There are no significant differences in wound closure percentages among the groups of 1-hour, 4-hour, and 24-hour post-burn debridement performed. f) Significant differences in sebaceous gland count were observed between sham wounds and burn wounds in scar tissue, with no notable variance detected across the three-time points of excision within the burn wound group.** $p<0.01$, ****$p<0.0001$.

Scar site of burn wounds reveals fewer sebaceous glands than sham wounds

This investigation aimed to discern the disparities in burn wound healing processes by comparing different burn areas. Initially, we established a baseline by conducting excisions of a uniform size, measuring 1.6 cm * 1.6 cm. Subsequently, we introduced a variation by including a group subjected to a smaller burn area of 1 cm * 1 cm. Through meticulous analysis, particularly in Figures 2a and 2b, we observed distinct differences in scar size and sebaceous gland density between sham and burn wounds, which the data were later quantified.

We employed ORO staining techniques to elucidate further the healing dynamics, scar formation, and sebaceous gland regeneration, as depicted in Figures 2c and 2d. This method

facilitated precise identification and visualization of sebaceous glands within scar tissue, enabling a comprehensive comparison of regenerative processes between the two wound types. Notably, Figure 2e underscored significant variations in scar size across sham wounds and various burn wound severities, highlighting unique scarring patterns associated with burn injuries.

Our findings revealed a compelling correlation, as illustrated in Figure 2f, between more extensive burn wound areas and decreased sebaceous gland counts. This sheds light on the intricate relationship between burn wound size and the regenerative capacity of sebaceous glands. Specifically, we observed less sebaceous gland regeneration in larger burn areas, indicating a significant difference in the regenerative process.

These results indicate that the burn area significantly influences scar formation and sebaceous gland regeneration, provides valuable contributions to understanding the complexities of burn wound healing, and may inform future therapeutic interventions to enhance tissue regeneration and minimize scarring.

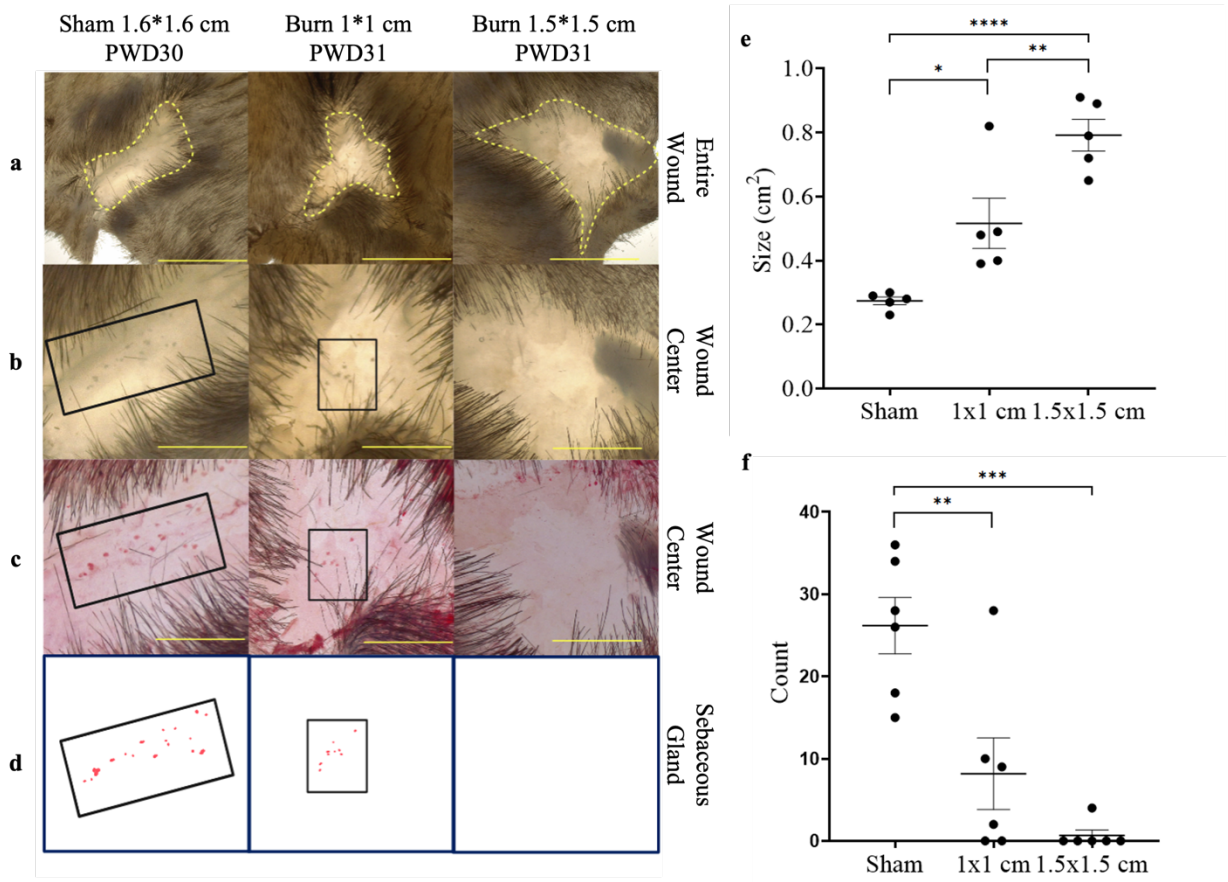

Figure 2: The scar site of burn wounds reveals fewer sebaceous glands than sham wounds, with a more prominent scar area. a.b) Tissues were cut in the same size (1.6x1.6 cm) with a different burn area and fixed before being observed under a microscope. Comparing the scar between sham and burn wounds, there is a significant difference between scar size and sebaceous gland count. c.d) Tissues were stained with Oil-Red O to identify sebaceous glands regenerated within the scar site, as found along the centerline of the scar. e) Although the wound size stayed consistent, a significant difference in scar size was measured among sham, 1x1 cm burn, and 1.5*1.5 cm burn. f) Less sebaceous glands were found in a larger burn wound, with mostly none in 1.5x1.5 cm burns. * $p<0.01$, ** $p<0.001$, *** $p<0.0001$**** $p<0.0001$.

Potential link of MyD88 and TRIF pathways with tissue regeneration mechanisms

The influence of immune cells, particularly macrophages and T cells, on the regeneration of mammalian hair follicles underscores the intricate interplay between the immune system and

tissue regeneration processes[13]. Additionally, the activation of Toll-like receptor 4 (TLR4) triggers distinct signaling pathways, MyD88 and TRIF, which have differential effects on the regulation of critical molecules in dendritic cells (DCs) and macrophages during lipopolysaccharide (LPS) stimulation.[14]. This suggests a potential link between immune signaling pathways and tissue regeneration mechanisms.

To investigate the contribution of these immune-related pathways to wound healing and sebaceous gland regeneration, experiments were conducted on MyD88-TRIF knockout mice. The results revealed a delayed wound-healing process compared to wild-type mice (Figure 3a). While burn wounds on WT mice are closed on day 18-20, only one of 5 MyD88-TRIF knockout mice burn wounds has closed by day 22. Data in Figure 3b also shows that since the beginning of the experiment, the process of MyD88-TRIF knockout mice burn would closure are slower. These data indicate these immune signaling adaptors' critical role in wound healing. Furthermore, the absence of sebaceous gland regeneration in MyD88-TRIF knockout mice suggests a potential involvement of immune pathways in regulating skin regeneration.

These findings highlight the importance of understanding the role of the adaptive immune system in wound healing and tissue regeneration processes. Enhancing immune-mediated mechanisms could hold promise for improving wound healing outcomes and promoting tissue regeneration, offering potential therapeutic strategies for addressing various skin-related

conditions. Further research into how immune signaling pathways can be targeted and modulated to enhance tissue regeneration may pave the way for innovative treatment approaches in regenerative medicine.

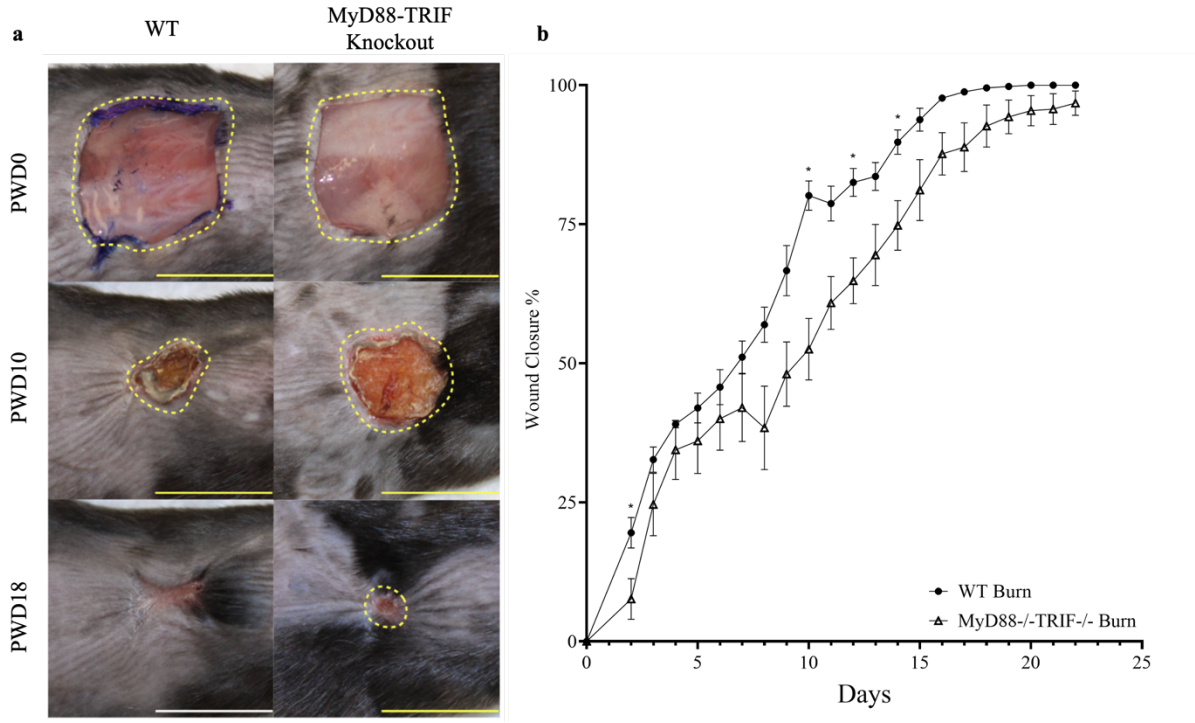

Figure 3: Burn wounds on MyD88-TRIF knockout mice have a delay in wound healing comparing to burn wounds on WT mice. a) Burn wound size comparison for two different groups: WT mice and MyD88-TRIF knockout mice. Pictures show changes in the wound at three time points: procedure day (Day 0), the most significant difference in closing rate (Day 10), and burn wound on WT mice fully closed (Day 18). b) Different wound closure rates of burn wounds on WT mice and MyD88-TRIF knockout mice from day 0 to day 22. After the procedure, the wound closure percentage started to significantly differ on day 2, with the most significant difference on day 10. Burn wounds on WT mice are all closed on day 20, while most burn wounds on MyD88-TRIF knockout mice are still open on day 22. * $p<0.01$.

Effect of D-MAP impact to burn wound regeneration compared to other hydrogel

The D-peptide crosslinked MAP hydrogel (D-MAP) elicited an antigen-specific immune response, demonstrating that biomaterial-induced adaptive immunity can drive cutaneous regenerative healing despite faster scaffold degradation[12]. By investigating the delayed wound healing and lack of sebaceous gland regeneration in MyD88-TRIF knockout mice compared to wild-type counterparts, we seek to underscore the critical involvement of immune pathways in tissue repair mechanisms. We aim to assess the immunogenicity and regenerative potential of D-peptide crosslinked MAP hydrogel (D-MAP) in promoting cutaneous healing, potentially offering insights into biomaterial-induced adaptive immunity in tissue regeneration.

Solosite™ is a widely applied commercial product and a pivotal component in biomaterials-based regenerative strategies for skin tissue wound healing[15]. Moreover, Solosite™'s widespread use underscores its efficacy and versatility in addressing various wound types, including burns, ulcers, and surgical wounds. As a critical player in biomaterial-based regenerative strategies, Solosite™ facilitates cell migration and proliferation, which is essential for restoring damaged skin tissue. According to findings from the study on hydrogel-based dressings for burn wounds in rats, Solosite™ demonstrated superior wound closure during treatment ($p<0.05$) and induced better results in the inflammatory and proliferative phases of healing compared to other hydrogel dressings ($p<0.05$). These results highlight Solosite™ as one

of the leading commercially available hydrogel products for promoting wound healing efficacy in experimental models[16].

Comparing D-MAP with Solosite™ for wound regeneration could provide valuable insights into the efficacy of these biomaterials in promoting skin tissue healing. While Solosite™ has established itself as a widely applied commercial product, praised for its ability to create an optimal healing environment and facilitate wound closure across various wound types, including burns and surgical wounds, D-MAP presents a novel approach with its D-peptide crosslinked MAP hydrogel composition. Despite scaffold degradation, the study demonstrating D-MAP's ability to elicit an antigen-specific immune response and drive cutaneous regenerative healing underscores its potential as an innovative biomaterial for wound regeneration.

To evaluate the efficacy of D-MAP, L-MAP, and Solosite™ in treating burn wounds, we conducted an experiment using a standardized burn wound model in mice. Each group received treatment with one of the three biomaterials, while a control group received no treatment. The aim was to assess these treatments' healing dynamics and comparative effectiveness in promoting skin tissue regeneration.

The treatment groups ' analysis of wound healing progression revealed distinct differences in healing rates. As shown in figure 4, by day 3 post-treatment, wounds treated with D-MAP showed the fastest healing, followed by those treated with Solosite™, while wounds treated with

L-MAP exhibited the slowest progress in wound closure. On day 7, statistical analysis demonstrated a significant difference between the D-MAP and Solosite™ groups regarding wound closure rates. Wounds treated with D-MAP exhibited accelerated healing compared to those treated with Solosite™. From day 10 onwards, a significant disparity in wound healing rates became apparent between the D-MAP and L-MAP treatment groups. Wounds treated with D-MAP demonstrated superior healing compared to those treated with L-MAP. Although no statistically significant difference was observed between the D-MAP and Solosite™ groups since day 10, it's noteworthy that wounds treated with D-MAP continued to heal faster. By day 26, two wounds in the D-MAP group had closed entirely, indicating the sustained efficacy of D-MAP in promoting wound closure. Despite variations in wound healing rates among the treatment groups, none of the experimental treatments facilitated sebaceous gland regeneration. This underscores the need for further research into strategies that promote wound closure and support full tissue regeneration, including restoring appendages such as sebaceous glands.

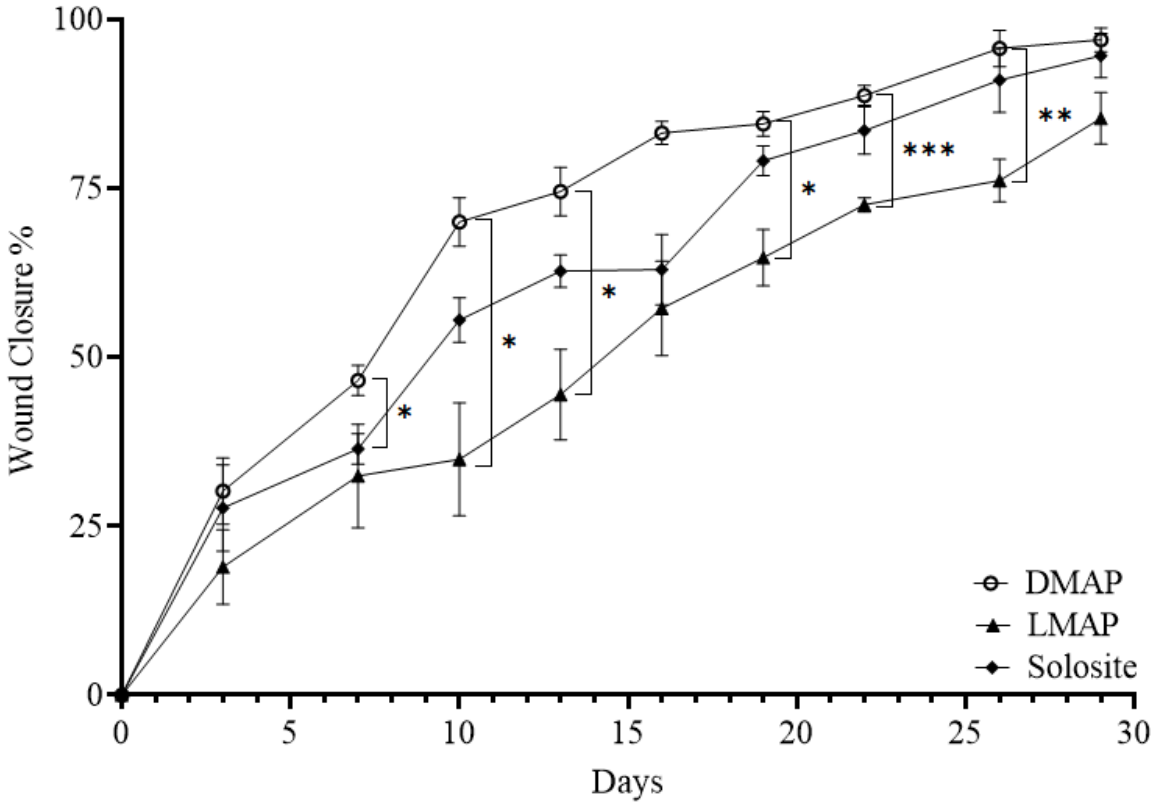

Figure 4: D-MAP shows a promising benefit to other hydrogel options. By day 3, D-MAP-treated wounds showed the fastest healing, followed by Solosite™, with L-MAP-treated wounds lagging. By day 7, D-MAP demonstrated superior healing over Solosite™. From day 10, D-MAP-treated wounds outpaced L-MAP. Though D-MAP continued faster healing until day 26, none of the treatments promoted sebaceous gland regeneration. * $p<0.01$, ** $p<0.001$, *** $p<0.0001$.

DISCUSSION

Unlike human skin, which lacks the apparent regeneration of sebaceous glands in excisional and burn wounds, mice exhibit a fascinating phenomenon wherein within large wounds wound-induced hair neogenesis (WIHN) leads to the regeneration of sebaceous glands in large excisional wounds[17], though not in burn wounds. The overall hope is that insights gleaned from this model can lead to improved ways to regenerate skin in humans following wounding. The complexity of this process hinges on intricate epithelial-mesenchymal cell interactions, predominantly influenced by Wnt signaling, while inflammation plays a pivotal role in tissue and hair follicle regeneration. By delving into these mechanisms in mice, we aim to gain deeper insights into the intricate dynamics of skin regeneration, thus potentially offering invaluable contributions to our understanding of human wound healing processes.

To further elucidate the underlying mechanisms driving the observed disparities in wound healing and hair follicle neogenesis between sham and burn mice, our focus extends to investigating various cell types that play pivotal roles in these processes. WIHN is a process in adult mammalian skin where fully functional hair follicles regenerate within large wounds, resembling embryonic hair development. Molecular mechanisms involving canonical WNT signaling, TLR3-mediated RNA sensing, and inflammatory cells, such as Fgf9-producing γ-δ T cells and macrophages, drive WIHN. This phenomenon showcases remarkable cellular plasticity,

involving multiple stem cell populations and lineage switching of differentiated cells, offering insights into mammalian development and potential clinical avenues for hair-related disorders and fibrotic scarring treatments[18]. Specifically, we would like to employ advanced techniques such as flow cytometry and single-cell RNA sequencing to dissect key cellular players' contributions to the wound tissue.

Through detailed flow cytometric analysis in the former study, the temporal dynamics of cellular composition in wounds are uncovered, highlighting the proliferation of epidermal cells and the persistent presence of various immune cells throughout the healing process. Moreover, specific permissive cell subpopulations within wounds are identified, offering crucial insights into the mechanisms underlying hair follicle neogenesis. Notably, the prolonged involvement of myeloid cells, such as monocytes and neutrophils, suggests their potential role in facilitating tissue remodeling and regeneration. The characterization of T cell populations challenges previous assumptions, highlighting the prevalence of CD8+ T cells expressing γδTCR and expanding our understanding of the immune response in wound healing and its impact on hair follicle regeneration[19].

Additionally, the latter study utilizing scRNA-seq data reveals critical evidence regarding the cellular and molecular dynamics underlying hair follicle regeneration during wound repair. The over-representation of upper wound fibroblasts, characterized by the expression of Crabp1,

in regenerative wound conditions indicates their pivotal role in promoting hair follicle regeneration. Furthermore, comparisons of fibroblast lineages between scarring and regenerating wounds elucidate distinct trajectories towards upper and lower wound fibroblasts, with the upper populations closely associated with specialized dermal papilla and sharing gene signatures akin to the murine papillary fibroblast lineage[20]. These findings, collectively, offer valuable groundwork for further research to apply these processes for therapeutic interventions in excisional wounds and potentially in burn wounds, thereby expanding our understanding of wound healing and hair regeneration across different injury types.

The delayed wound healing observed in burn wounds of MyD88-TRIF knockout mice underscores the intricate interplay between the Toll-like receptor (TLR) signaling pathway and immune cell function in the wound healing. MyD88, a crucial adaptor molecule in the TLR signaling cascade, is pivotal in orchestrating innate immune responses. The diminished wound healing in MyD88-TRIF deficient mice suggests the significance of TLR-mediated signaling pathways in regulating critical aspects of tissue repair. Given the diverse roles of immune cells in wound healing, particularly macrophages and dendritic cells (DCs), further investigation into their involvement is warranted. Macrophages, with their dual functions in phagocytosis and cytokine production, are integral to the inflammatory and proliferative phases of wound healing. The heterogeneous phenotypes of macrophages, transitioning from pro-inflammatory to

reparative states, likely rely on TLR signaling for appropriate activation and function. Similarly, DCs, known for their antigen presentation and cytokine production, may contribute to the early inflammatory responses crucial for initiating wound repair[21]. Understanding the precise roles of macrophages and DCs in TLR signaling could offer valuable insights into potential therapeutic strategies for enhancing wound healing processes, particularly in conditions associated with dysregulated immune responses like burn injuries.

The utilization of MAP gel, particularly D-peptide crosslinked MAP hydrogel (D-MAP), presents a promising avenue for enhancing wound healing through the modulation of immunological responses. By harnessing the ability of MAP gel to recruit immune cells crucial for tissue repair, this study underscores its potential in addressing the complex challenges of burn wound healing. However, while the results highlight the efficacy of MAP gel in promoting cutaneous regeneration, further investigation into its application, specifically in burn wound contexts, is warranted. Understanding the intricate interplay between MAP gel-induced immune responses and burn wound pathophysiology could unveil novel therapeutic strategies for optimizing burn wound management.

In contrast to established commercial products like Solosite™, the experimental data demonstrate that D-MAP exhibits superior outcomes in promoting wound closure and healing dynamics. This challenges the conventional notion of efficacy associated with widely used

products and underscores the importance of exploring innovative biomaterials for wound management. The findings suggest that D-MAP may offer a more effective alternative for burn wound treatment, highlighting the potential of novel approaches to surpass existing standards of care and improve patient outcomes.

Ultimately, the overarching goal of wound healing research is to develop products that not only accelerate wound closure but also support comprehensive tissue regeneration. The study's findings position D-MAP as a promising candidate in advancing this objective, offering hope for individuals suffering from burn injuries. By pushing the boundaries of conventional wound management approaches and prioritizing the development of innovative therapies, this research contributes to the ongoing efforts to address the unmet needs of burn patients and improve their quality of life.

CONCLUSION

Our study delved into the intricate mechanisms governing wound healing, primarily focusing on full-thickness burns and the interplay between immune signaling pathways and tissue regeneration. The investigation commenced by highlighting the severity of full-thickness burns, emphasizing the importance of early excision interventions in optimizing patient outcomes and fostering expedited wound healing.

Through experimentation utilizing mouse models, we aimed to bridge the gap between human and murine skin regeneration processes, mainly focusing on wound-induced hair neogenesis and the role of immune signaling pathways such as Toll-like receptor (TLR) pathways in tissue repair. Our findings unveiled fascinating insights into the delayed wound healing observed in burn injuries and its correlation with the absence of sebaceous gland regeneration, a phenomenon observed in mouse models but notably absent in human burn wounds.

Further exploration into the immune-related pathways, particularly the MyD88 and TRIF pathways, underscored their pivotal role in wound healing and sebaceous gland regeneration. The delayed wound closure observed in MyD88-TRIF knockout mice highlighted the intricate interplay between immune responses and tissue regeneration mechanisms, suggesting potential targets for therapeutic intervention.

Moreover, our study on biomaterial-based treatments, specifically D-peptide crosslinked MAP hydrogel (D-MAP), demonstrated promising outcomes in promoting wound closure and facilitating cutaneous regeneration. Despite its accelerated scaffold degradation, D-MAP showed superior efficacy to established commercial products like Solosite™, challenging conventional notions of wound management efficacy and highlighting the potential of novel approaches in burn wound treatment.

Ultimately, the findings presented in this thesis offer valuable insights into the dynamics of wound healing post-burn injury and the potential avenues for therapeutic intervention. By pushing the boundaries of conventional wound management approaches and prioritizing the development of innovative therapies, this research contributes to the ongoing efforts to address the unmet needs of burn patients and improve their quality of life.

Further research is warranted to elucidate the mechanisms underlying D-MAP's efficacy and its application in burn wound contexts. Additionally, continued exploration of immune signaling pathways and their modulation may offer new insights and therapeutic strategies for enhancing wound healing processes in conditions associated with dysregulated immune responses, such as burn injuries.

We present a significant step forward in understanding the complex interplay between immune responses, tissue regeneration mechanisms, and novel biomaterial-based treatments in

burn wound management. The results offer the possibility for improved clinical outcomes and enhanced quality of life for individuals suffering from burn injuries.

REFERENCES

1. Żwierełło, W., et al., *Burns: Classification, Pathophysiology, and Treatment: A Review.* Int J Mol Sci, 2023. **24**(4).

2. Warby, R. and C.V. Maani, *Burn Classification*, in *StatPearls*. 2024: Treasure Island (FL).

3. *ISBI Practice Guidelines for Burn Care.* Burns, 2016. **42**(5): p. 953-1021.

4. Anyanwu, J.A. and R. Cindass, *Burn Debridement, Grafting, and Reconstruction*, in *StatPearls*. 2024: Treasure Island (FL).

5. Yousef, H., M. Alhajj, and S. Sharma, *Anatomy, Skin (Integument), Epidermis*, in *StatPearls*. 2024: Treasure Island (FL).

6. Hoover, E., S. Aslam, and K. Krishnamurthy, *Physiology, Sebaceous Glands*, in *StatPearls*. 2024: Treasure Island (FL).

7. Wang, X., et al., *Principles and mechanisms of regeneration in the mouse model for wound-induced hair follicle neogenesis.* Regeneration (Oxf), 2015. **2**(4): p. 169-181.

8. Bielefeld, K.A., S. Amini-Nik, and B.A. Alman, *Cutaneous wound healing: recruiting developmental pathways for regeneration.* Cell Mol Life Sci, 2013. **70**(12): p. 2059-81.

9. Dasu, M.R. and R. Rivkah Isseroff, *Toll-Like Receptors in Wound Healing: Location,*

Accessibility, and Timing. Journal of Investigative Dermatology, 2012. **132**(8): p. 1955-1958.

10. Macedo, L., et al., *Wound healing is impaired in MyD88-deficient mice: a role for MyD88 in the regulation of wound healing by adenosine A2A receptors.* Am J Pathol, 2007. **171**(6): p. 1774-88.

11. Griffin, D.R., et al., *Accelerated wound healing by injectable microporous gel scaffolds assembled from annealed building blocks.* Nat Mater, 2015. **14**(7): p. 737-44.

12. Griffin, D.R., et al., *Activating an adaptive immune response from a hydrogel scaffold imparts regenerative wound healing.* Nat Mater, 2021. **20**(4): p. 560-569.

13. Rahmani, W., S. Sinha, and J. Biernaskie, *Immune modulation of hair follicle regeneration.* npj Regenerative Medicine, 2020. **5**(1): p. 9.

14. Shen, H., et al., *Dual signaling of MyD88 and TRIF is critical for maximal TLR4-induced dendritic cell maturation.* J Immunol, 2008. **181**(3): p. 1849-58.

15. Kaur, G., et al., *Biomaterials-Based Regenerative Strategies for Skin Tissue Wound Healing.* ACS Applied Bio Materials, 2022. **5**(5): p. 2069-2106.

16. Bernardes, M.J.C., et al., *Hydrogel-based dressings in the treatment of partial thickness experimentally induced burn wounds in rats.* Acta Cir Bras, 2022. **37**(4): p. e370401.

17. Xue, Y., et al., *Wound-Induced Hair Neogenesis Model.* J Invest Dermatol, 2022.

142(10): p. 2565-2569.

18. Wier, E.M. and L.A. Garza, *Through the lens of hair follicle neogenesis, a new focus on mechanisms of skin regeneration after wounding.* Semin Cell Dev Biol, 2020. **100**: p. 122-129.

19. Helm, M., et al., *Cell Population Dynamics in Wound-Induced Hair Follicle Neogenesis Model.* Life (Basel), 2022. **12**(7).

20. Phan, Q.M., et al., *Single-cell transcriptomic analysis of small and large wounds reveals the distinct spatial organization of regenerative fibroblasts.* Exp Dermatol, 2021. **30**(1): p. 92-101.

21. Chen, L. and L.A. DiPietro, *Toll-Like Receptor Function in Acute Wounds.* Adv Wound Care (New Rochelle), 2017. **6**(10): p. 344-355.